Metallophysics and Advanced Technologies
Металофіз. новітні технол.
Metallofiz. Noveishie Tekhnol.
2024, vol. 46, No. 6, pp. 549–557
https://doi.org/10.15407/mfint.46.06.0549
Reprints available directly from the publisher

PACS numbers: 68.35.Ja, 68.37.Hk, 68.37.Vj, 68.47.Gh, 78.30.Hv, 81.15.Pq, 82.45.Qr

Correlation between Structural, Morphological and Hydrophobic Properties of MgO Coating of Aluminium Substrate

Zehira Belamri

Phase Transformation Laboratory,
Department of Physics,
Frères Mentouri of Constantine 1 University,
DZ-25000 Constantine, Algeria

In this work, we investigate how the molarity of the solution affects the physical characteristics of MgO coatings. By oxidizing simply thermally magnesium that had been electrodeposited on aluminium substrates, stable MgO thin films are produced. The samples are characterized by x-ray diffraction (XRD), Raman spectroscopy, and scanning electron microscopy (FEG-SEM) equipped with energy dispersive x-ray analysis (EDX), a profilometer. The wettability properties of the synthesized films are estimated by measuring the contact angle between the surface of the films and a deposited water drop (WCA). The optimal MgO nanostructure coating crystallizes when magnesium layers are electroplated with 0.2 M of the solution for two hours at 500°C. The MgO-coating crystal orientation is influenced by the molarity of the solution. Data from the XRD analysis are corroborated by Raman-spectroscopy results. Normal vibrational modes, which are compatible with the MgO structure, are visible in the acquired spectra. The study findings suggest that the vibrational mode of the MgO coating described in this work is affected by changing the solution molarity. This form may be responsible for the $MgO_{0.2}$ layer best hydrophobicity, which is caused by air trapping between the nanowires (fibres) to prevent water from clinging to the film.

Key words: MgO coating, aluminium substrate, molarity, electroplating, best hydrophobicity, nanowires.

У цій роботі було досліджено, як молярність розчину впливає на фізичні характеристики покриттів MgO. Шляхом простого термічного окиснення

Corresponding author: Belamri Zehira
E-mail: belamri.zehira@umc.edu.dz

Citation: Zehira Belamri, Correlation between Structural, Morphological and Hydrophobic Properties of MgO Coating of Aluminium Substrate, *Metallofiz. Noveishie Tekhnol.*, **46**, No. 6: 549–557 (2024). DOI: 10.15407/mfint.46.06.0549

маґнію, який був електроосаджений на алюмінійові основи, було одержано стабільні тонкі плівки MgO. Зразки були досліджені методами рентґенівської дифракції, Раманової спектроскопії та сканувальної електронної мікроскопії з використанням енергодисперсійної рентґенівської аналізи, профілометра. Змочуваність синтезованих плівок оцінювали шляхом міряння кута контакту між поверхнею плівок і краплею води, що осаджується. Оптимальне наноструктурне покриття MgO кристалізується під час ґальванічного осадження шарів маґнію 0,2 М-розчином протягом двох годин за температури у 500°C. На кристалічну орієнтацію покриття MgO впливає молярність розчину. Дані рентґеноструктурної аналізи підтверджуються результатами спектроскопії комбінаційного розсіяння світла. В одержаних спектрах було помітно нормальні коливні моди, сумісні зі структурою MgO. Результати дослідження уможливлюють припустити, що описана в цій роботі форма коливань покриття MgO залежить від зміни молярности розчину. Ця форма може бути відповідальною за найліпшу гідрофобність шару $MgO_{0.2}$, що зумовлена утримуванням повітря між нанодротами (волокнами), яке запобігає прилипанню води до плівки.

Ключові слова: покриття MgO, алюмінійова підкладинка, молярність, ґальванічне покриття, найліпша гідрофобність, нанодроти.

(Received 7 February, 2024; in final version, 11 April, 2024)

1. INTRODUCTION

Many inorganic materials have been investigated as effective anticorrosive coating components and corrosion inhibitors for a number of metallic substrates that are susceptible to environmental corrosion such as NaCl solution, fuel oil, simulated body fluid, and gas turbine environments [1]. One of the best ways to inhibit corrosion on metal surfaces is to form a passivation coating [2, 3]. Wettability, or the surface affinity for water, is the most significant property of this coating material. As a measure of a surface wettability, hydrophobicity is determined by its chemical composition, structure, morphology, and the contact angle (CA) that a liquid has with the surface. These characteristics allow surfaces to be categorized into various domains, including superhydrophilic ($CA = 5°$ in 0.5 sec), hydrophilic ($CA = 90°$), hydrophobic ($CA > 90°$), and superhydrophobic ($CA = 150°–180°$) [4–14]. Several materials are used in this field of application, such as ZnO [15–20]. Magnesium oxide (MgO) is chosen in this present work for deposition as a thin film on aluminium substrate due to its excellent physical and non-toxicology properties. Magnesium oxide thin films have significant application features that are generating a lot of interest in science and technology [21]. These films find wide applications in solar cells, photodetectors, light-emitting diodes, optoelectronic devices, and sensors [22, 23]. MgO exhibits exceptional band gap characteristics with chemical and thermal stability [21, 22].

In recent years, a number of techniques have been developed for the fabrication of magnesium oxide (MgO) thin films and coatings. These techniques include pulsed-laser deposition (PLD), magnetron sputtering, electron beam evaporation, metal organic chemical vapour deposition (MOCVD), and spray pyrolysis [24–29]. Nonetheless, the choice of synthesis process is contingent upon the particular demands of the application, the intended film thickness, uniformity, and surface states, in addition to the equipment and resources at hand. By varying the electrolyte composition and applied voltage, the electrodeposition approach offers appropriate and controllable methods for generating composite films on a variety of diverse substrates [30]. Furthermore, it is the most widely used and reasonably priced method of producing surface roughness on metal. It has been shown that water-repellent coatings on aluminium substrates vary in their wetting qualities, durability, roughness, and anti-icing ability [31].

The present work is a new one where we have investigated the impact of the solution molarity on the structural, morphological, and hydrophobic properties of MgO thin films deposited on aluminium substrate using a low-cost electrodeposition method without adding corrosion inhibitors or surface modifications, which are expensive and can lead to toxicity and environmental issues.

2. EXPERIMENTAL DETAILS

2.1. Substrate Preparation and Deposition of Thin Films

In the current work, pure aluminium is utilized as the substrate; to achieve a flat shape with a thickness of roughly 2 mm, it must be mechanically polished using abrasive paper. Preparing for usage, the substrates were cleaned using distilled water and methanol for 15 minutes each in ultrasonic baths. For the deposition of MgO thin films, an aqueous solution of 0.1 M and 0.2 M magnesium nitrate ($Mg(NO_3)_2$–$6H_2O$) precursor was dissolved in distilled water. A cleaned aluminium substrate is used as a cathode and the platinum plate as an anode; both electrodes were vertically immersed in the as-prepared solution and kept at a distance of 1.5 cm. A voltage of −10 V DC was applied for 15 minutes. In order to guarantee the complete oxidation of Mg, after deposition, the thin Mg layers were annealed at 500°C for 2 hours.

2.2. Characterization

The structural properties of the as-prepared samples were determined using a PANALYTICAL empyrean diffractometer (XRD, $\lambda_{Cu} = 1.540$

Å). The data from XRD were examined using X'Pert High Score software. The Raman spectra were measured on a HORIBA LabRAM HR Evolution spectrometer at room temperature with a monochromatic light source of 473 nm. The morphological and elemental analyses were executed using a Field Emission Gun Scanning Electron Microscope (FEG-SEM, JEOL FEG JSM-7100F) equipped with an energy dispersive x-ray spectrometer (EDS). The measurement of the water contact angle (WCA (θ)) has been used to determine the surface wettability of the elaborated MgO thin films. A light source of the LEYBOLD type (6 V, 30 W) was used for lighting and projecting the drops' image onto the sample, together with a projection lens that allowed the image to be magnified onto a transparent screen of dimensions 30×30 cm^2.

3. RESULTS AND DISCUSSIONS

3.1. Structural Studies

The structure of the elaborated MgO coating has been identified by x-ray diffractometer, using the existing databases in the form of ICSD cards No.: 96-901-3200. The samples were analysed between 20° and 80° diffraction angles at room temperature. The XRD spectra show the different diffraction peaks observed at $2\theta = 38.45°$, 44.66°, 65.07° and 78.22°, which are attributed respectively to the (111), (020), (022) and (131) lattice planes of the MgO structure (Fig. 1), and which check the successful elaboration of MgO thin films. For the $MgO_{0.1}$ sample, the

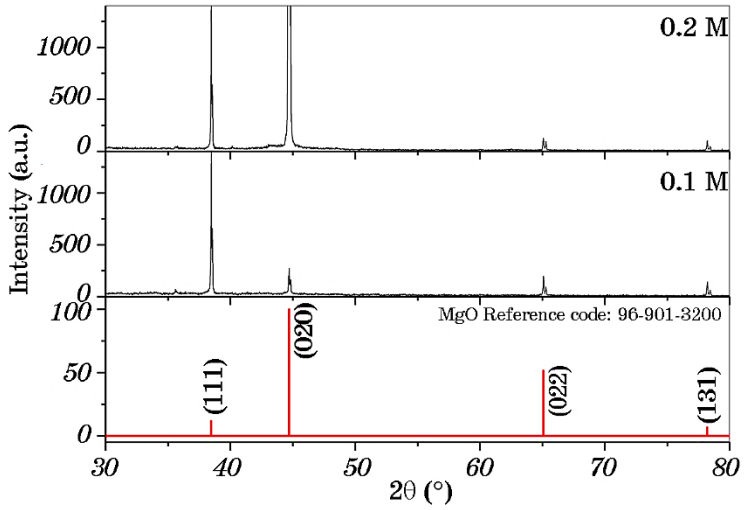

Fig. 1. X-ray diffraction spectra of elaborated MgO thin films (the molarity of solution is indicated inside the figures).

dominant peak is (111) and with varying the solution molarity to 0.2 M, the crystal orientation changes with the (020) peak. The sharpest peaks with the greatest intensities sign a good crystallinity and a larger grain boundary dimension [32, 33]. The migration of molecules onto a growing surface may provide an explanation for the observed link between the degree of preferred orientation and the molarity of the solution. It is believed that when nucleating, MgO will attain a favoured orientation of (020) with a lower energy configuration. A change in crystallite size can also account for this difference in the analysed sample peak intensities. Scherrer's formula [34] has been applied to calculate the crystallite size of the MgO thin film, using the full width at half maximum (FWHM) of the highly oriented peak (020) located around 44.65° in the XRD spectrum (Fig. 1):

$$D = \frac{0.9\lambda}{\beta \cos\theta}, \tag{1}$$

where $\lambda = 0.1540$ nm—x-ray wavelength, θ—Bragg-diffraction angle, and β—FWHM.

Table 1 summarizes the position of the (020) peak and estimated crystallite size. The obtained results reveal that the crystallite size is on the nanometric scale. The crystallite size decreases from 144 nm for the $MgO_{0.1}$ thin film to 115 nm for the $MgO_{0.2}$ sample.

Until now, the interpretation of the Raman spectrum of MgO is not clear, but we will try to base it on some previous results to understand the origin of the vibration modes appearing on the Raman spectra of the samples studied in this present work. It was found that the Raman modes of MgO compounds were dependent on their size and shape, while other modes were rather constant and identified as surface phonon modes [35]. Visweswaran *et al.* [36] reported that, from group theory, the Raman active modes are as follow:

$$T_{1u} x T_{1u} = A_{1a} + E_a + T_{1a} + T_{2a}. \tag{2}$$

In this work, the Raman spectra of the elaborated MgO coating are shown in Fig. 2. For $MgO_{0.2}$, six Raman peaks appear around 137, 487,

TABLE 1. Structural parameters of elaborated MgO thin films as a function of the solution molarity

Sample	$2\theta_{020}$ (°)	FWHM (°)	Crystallite size D (nm)	Dislocation density $\delta \times 10^{14}$ (line/m^2)	Lattice deformation ($\varepsilon \times 10^{-3}$)
$MgO_{0.1}$	44.7087	0.0624	144	0.484	0.252
$MgO_{0.2}$	44.6421	0.0780	115	0.756	0.315

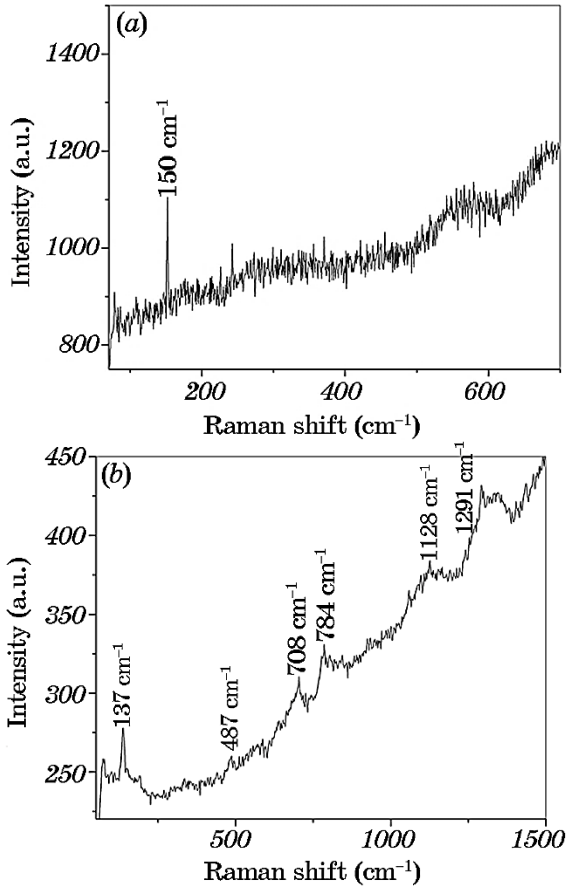

Fig. 2. Raman spectra of the MgO thin films on aluminium substrate: $MgO_{0.1}$ (*a*), $MgO_{0.2}$ (*b*).

708, 784, and 1128 cm^{-1}. The vibrational modes at 137 cm^{-1} similar to those of ZnO named E_2^{low} [19, 20], can be associated with the vibration of the lattice of Mg atoms. The band centred at 487 cm^{-1} is designated E_2^{high} first-order Raman modes [36]. In the spectrum of MgO, second-order Raman bands appear around 1088 cm^{-1} [37]. In this work, band around 708, 784, 1128 and 1300 cm^{-1} may be related to the second-order Raman modes.

3.2. Morphological and Wettability Studies

Different atomic rearrangement processes involved during the thermal oxidation of MgO thin films obtained with different molarity on the aluminium substrates are responsible for the different surface

morphologies of these studied layers.

Figure 3 shows the micrographs obtained by the Field Emission Gun Scanning Electron Microscope (FEG–SEM) of these samples. It is clearly appearances that the $MgO_{0.1}$ film morphology is asymmetrical and flaky (Fig. 3, *a*). Hence, with the increase of the solution molarity, the morphology of MgO films changes. The $MgO_{0.2}$ sample presents the nanowires (fibres), which are dispersed homogeneously and all over the films surface. This morphology may be responsible for the best hydrophobicity of the $MgO_{0.2}$ layer, where air trapping between the nanowires (fibres) prevents water from adhering to the film. Compacted

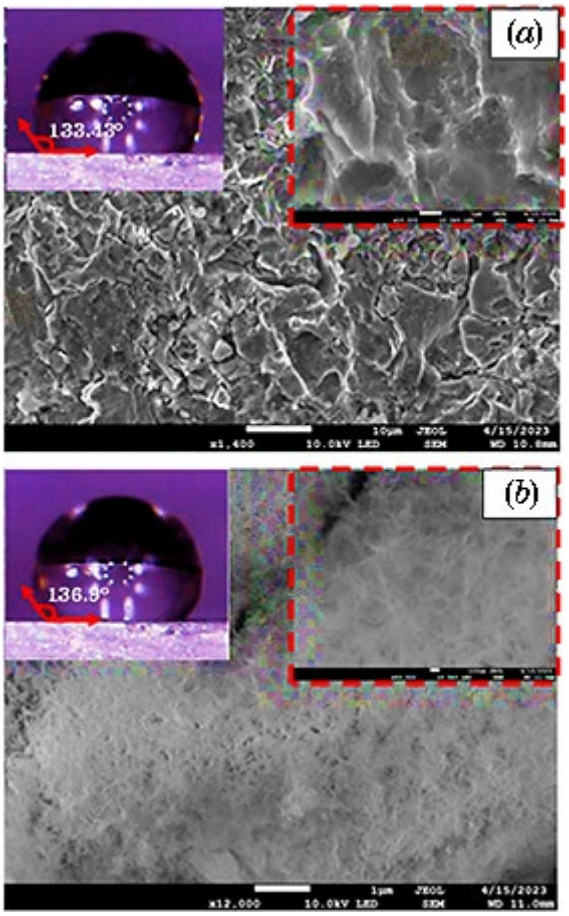

Fig. 3. FEG-SEM images of MgO thin films: $MgO_{0.1}$ (inset right image shows the nanowires with a High-magnification, and left image shows contact angle of the water drops) (*a*), $MgO_{0.2}$ (inset right image shows the nanowires with a High-magnification, and left image shows contact angle of the water drops) (*b*).

fibres that cover the $MgO_{0.2}$ surface lead to a hydrophobic surface with a WCA of 136.93°.

4. CONCLUSION

In this work, we performed a study on the impact of the solution molarity on the physical properties of MgO coatings. Stable MgO thin films were obtained by simple thermal oxidation of electrodeposited Mg on aluminium substrates.

The treatment for 2 h at 500°C of electroplating Mg layers with 0.2 M of the solution, leads to the best crystallization of the MgO nanostructure coating. The solution molarity has an effect on the crystal orientation of MgO coating.

Results from Raman spectroscopy support those from the XRD analysis. The obtained spectra showed normal vibrational modes that are consistent with the MgO structure. The study results indicate that increasing the solution molarity has an impact on the vibration mode of the MgO coating elaborated in this work.

The $MgO_{0.2}$ layer optimal hydrophobicity, which results from air trapping between the nanowires (fibres) to keep water from sticking to the film, may be attributed to this shape.

REFERENCES

1. P. Banerjee, R. Hasda, M. Murmu, and H. Hirani, *Anti-Corros Method* (Elsevier: 2022).
2. L. Feng, Y. Che, Y. Liu, Z. Yan, Y. Wang, and X. Qiang, *Surf. Interface Anal.*, **48**: 1320 (2016).
3. S. Zheng, C. Li, Q. Fu, W. Hu, T. Xiang, Q. Wang, M. Du, X. Liu, and Z. Chen, *RSC Adv.*, **6**: 79389 (2016).
4. K. Manoharan and S. Bhattacharya, *J. Manuf. Process.*, **2**: 59 (2019).
5. H. Gau, S. Herminghaus, P. Lenz, and R. Lipowsky, *Science*, **283**: 46 (1999).
6. N. Labbortt, J. P. Folkers, and G. M. Whitesides, *Science*, **257**: 1317 (1992).
7. P. Lenz, *Adv. Mater.*, **11**: 1531 (1999).
8. S. Abbott, J. Ralston, G. Reynolds, and R. Hayes, *Langmuir*, **15**: 8923 (1999).
9. D. Yoo, S. S. Shiratori, and M. F. Rubber, *Macromolecules*, **31**: 4309 (1998).
10. L. Jiang, R. Wang, B. Yang, T. J. Li, D. A. Tryk, A. Fujishima, K. Hashimoto, and D. B. Zhu, *Pure Appl. Chem.*, **72**: 73 (2009).
11. M. H. Hui and M. J. Blunt, *J. Phys. Chem. B*, **104**: 3833 (2000).
12. W. Chen, A. Y. Fadeev, M. C. Hsieh, D. Oner, J. Youngblood, and T. J. McCarthy, *Langmuir*, **15**: 3395 (1999).
13. J. P. Youngblood and T. J. McCarthy, *Macromolecules*, **32**: 6800 (1999).
14. D. Oner and T. J. McCarthy, *Langmuir*, **16**: 7777 (2000).
15. S. Patra, S. Sarkar, S. K. Bera, R. Ghosh, and G. K. Paul, *J. Phys. D: Appl. Phys.*, **42**: 075301 (2009).
16. Y. Li, M. Zheng, L. Ma, M. Zhong, and W. Shen, *Inorg. Chem.*, **47**: 3140 (2008).

17. N. Mufti, D. Arista, M. Diantoro, A. Fuad, A. Taufiq, and Sunaryono, *IOP Conf. Ser.: Mater. Sci. Eng.*, **202**: 012006 (2017).
18. G. Kenanakis, D. Vernardou, and N. Katsarakis, *Applied Catalysis A: General*, **411–412**: 7 (2012).
19. Zehira Belamri, W. Darenfad, and N. Guermat, *J. Nano-Electron. Phys.*, **15**: 02026 (2023).
20. Zehira Belamri, Leila Boumaza, Smail Boudjadar, *Phys. Scr.*, **98**: 125949 (2023).
21. G. Carta, N. El Habra, L. Crociani, G. Rossetto, P. Zanella, A. Zanella, G. Paolucci, D. Barreca, and E. Tondello, *Chem. Vap. Depos.*, **13**: 185 (2007).
22. A. M. Ezhil Raj, L. C. Nehru, M. Jayachandran, and C. Sanjeeviraja, *Cryst. Res. Technol.*, **42**: 867 (2007).
23. S. Visweswaran, R. Venkatachalapathy, M. Haris, and R. Murugesan, *J. Mater. Sci. Mater. Electron.*, **31**: 14838 (2020).
24. T. Ishiguro, Y. Hiroshima, and T. Inoue, *Jpn. J. Appl. Phys.*, **33**: 3537 (1996).
25. I. Shih, S. L. Wu, L. Li, C. X. Qiu, P. Grant, and M. W. Denhoff, *Mater. Lett.*, **11**: 161 (1991).
26. J. Talacchio, G. R. Wagner, and H. C. Pohl, *Physica C*, **659**: 162 (1989).
27. Z. Lu, R. S. Feigelson, R. K. Route, S. A. Di Carolis, R. Iliskes, and R. D. Jacowitz, *J. Cryst. Growth*, **128**: 788 (1993).
28. X. Yi, W. Wenzhong, Q. Yitai, Y. Li, and C. Zhiwen, *Surf. Coat. Technol.*, **82**: 291 (1996).
29. Y. Lee, H. Kim, and Y. Roh, *Jpn. J. Appl. Phys.*, **40**: 2423 (2001).
30. M. Moradi, R. Saidi, B. Hoomehr, and K. Raeissi, *Ceram. Int.*, **49**: 9239 (2023).
31. F. J. Montes Ruiz-Cabello, P. Ibacez-Ibacez, G. Paz-Gomez, M. Cabrerizo-Vilchez, and M. A. Rodriguez-Valverde, *J. Vis. Exp.*, **138**: e57635 (2018).
32. P. M. Perillo, M. N. Atia, and D. F. Rodríguez, *Rev. Mater.*, **23**, No. 2: e-12133 (2018).
33. M. F. Malek, M. H. Mamat, M. Z. Sahdan, M. M. Zahidi, Z. Khusaimi, and M. R. Mahmood, *Thin Solid Films*, **527**: 102 (2013).
34. G. Kenanakis, E. Stratakis, K. Vlachou, D. Vernardou, E. Koudoumas, and N. Katsarakis, *Appl. Surf. Sci.*, **254**: 5695 (2008).
35. M. Dekermenjian, A. Peter Ruedige, and A. Merlen, *RSC Adv.*, **13**: 26683 (2023).
36. S. Visweswaran, R. Venkatachalapathy, M. Haris, and R. Murugesan, *J. Mater. Sci. Mater. Electron.*, **31**: 14838 (2020).
37. J. P. Singh and L. Gupta, *Int. J. Math. Eng. Manag. Sci.*, **4**: 619 (2019).